

The Phenomenon of Steady-State String Motion

R. Miroshnik

Expert Researcher,
The Israel Electric Corporation, Ltd.
R&D Division,
Amir Bldg.
Haifa 31000, Israel
e-mail: mir@iec.co.il

The paper examines the phenomenon of steady-state motion for a string traveling with constant velocity along an invariant curve under gravity in a viscous medium. This technically important phenomenon has been known in the literature for about 120 years and may be applied in high-speed turbines, the textile industry, etc. The conditions for the phenomenon's existence are found. Concepts of two critical string velocities as well as sub, super, and hypercritical domains are introduced. The analytical solutions for the nonlinear differential equations and arbitrary constants for the general boundary conditions are found. The theoretical results are very close to the experimental ones.
[DOI: 10.1115/1.1380677]

1 Introduction

The paper examines the technically important phenomenon of a steady-state string traveling with constant velocity along an invariant curve (mode) under gravity in a viscous medium. The phenomenon is illustrated schematically in Fig. 1. The string comes out from outlet device 2 (outlet), moves along invariant mode 1 or 4, and enters into inlet device 3 (inlet). One sees the string frozen in space, because the motion along the mode is invisible. The string in fact moves only along itself and its velocity at every point is constant and directed to the mode tangent. This phenomenon may be applied in high-speed turbines cooling, thread coiling in the textile industry, design of easily unrolled mobile radio antennas, etc.

This problem has a long research history and still no complete solution. In the last century Aitkin [1] and Radinger [2] wrote about the string "rigidity" that in their opinion is produced by the centrifugal forces. Smith and Weathezhon [3] and Burge [4] examined the phenomenon's heat exchange for practical use in high-speed turbine cooling. Voevodin [5] had carried out numerous experiments with different textile cords elevation up to the height of 30 m.

Kurkin and Lebedev [6] showed experimentally in a vacuum chamber that the phenomenon ceases to exist when the air is removed. A heavy metallic cord was also elevated due to its specially heightened aerodynamic resistance. These experiments showed that a dominant reason for the phenomenon's existence is the friction of string-on-air.

Svetlicky and Gabruk [7], Cohen and Epstein [8], and Nordenholz and O'Reilly [9] examined the kinematical conditions of steady-state string motion. Svetlicky and Miroshnik [10], Kurkin and Miroshnik [11], Healey and Papadopoulos [12], and Schagerl et al. [13] analyzed different particular cases of string traveling. Perkins and Mote [14,15] analyzed the vibration and stability conditions of traveling cables while neglecting the resistance of the medium.

The purposes of this paper are to present analytical solutions of the above boundary value problem for different domains of string traveling when considering the resistance of the medium and compare these solutions with the experiment results. The analyses below and given discussion of the results provide the explanation for the phenomenon's existence.

Contributed by the Applied Mechanics Division of THE AMERICAN SOCIETY OF MECHANICAL ENGINEERS for publication in the ASME JOURNAL OF APPLIED MECHANICS. Manuscript received by the ASME Applied Mechanics Division, May 23, 2000; final revision, November 18, 2000. Editor: N. C. Perkins. Discussion on the paper should be addressed to the Editor, Prof. Lewis T. Wheeler, Department of Mechanical Engineering, University of Houston, Houston, TX 77204-4792, and will be accepted until four months after final publication of the paper itself in the ASME JOURNAL OF APPLIED MECHANICS.

2 The Differential Equations

We assume that a homogeneous, inextensible, ideally flexible string without bending and torsional stiffness travels with a constant velocity along an invariant mode having length L . Gravity and resistance of the medium (drag force) load the string. The drag force is assumed as constant, always directed along the mode tangentially opposite to the traveling velocity. The differential equations of the steady-state plane motion may be derived ([7]) from "equilibrium" of string element shown in Fig. 2. The equations' derivation in general form is given in the Appendix. These equations in projections onto Cartesian coordinates X, Y in nondimensional form are

$$\begin{aligned} \frac{d}{ds} \left(p^* \frac{dx}{ds} \right) - \frac{dx}{ds} &= 0; \\ \frac{d}{ds} \left(p^* \frac{dy}{ds} \right) - \frac{dy}{ds} - n &= 0; \\ \left(\frac{dx}{ds} \right)^2 + \left(\frac{dy}{ds} \right)^2 &= 1, \end{aligned} \quad (1)$$

where the nondimensional variables x, y, s, p^*, n are equal to

$$x = \frac{X}{L}; \quad y = \frac{Y}{L}; \quad s = \frac{S}{L}; \quad p^* = \frac{P^*}{m\mu L}; \quad n = \frac{g}{\mu};$$

$P^* = P - mV^2$ is the fictitious string tension; P is the real tension; V is the traveling velocity; and μ is the drag force of the string unit mass (acceleration). The drag force that depends on the string geometry and material, medium viscosity, etc., ([6]) increases monotonically with the traveling velocity; g is the gravity acceleration; m is the string linear mass; and S is the arc (Euler) coordinate along the mode.

The fictitious tension P^* may have any sign, however, the real tension P is assumed to be positive.

3 Equations' Analytical Solution

Integrating the first of Eq. (1) gives

$$p^* \frac{dx}{ds} - x = C_1. \quad (2)$$

Substitution of p^* from Eq. (2) into the second Eq. (1) in terms of

$$\frac{d}{ds} = \frac{dx}{ds} \frac{d}{dx}; \quad ds = \pm dx \sqrt{1 + \left(\frac{dy}{dx} \right)^2} \quad (3)$$

yields (while considering the sign plus of ds)

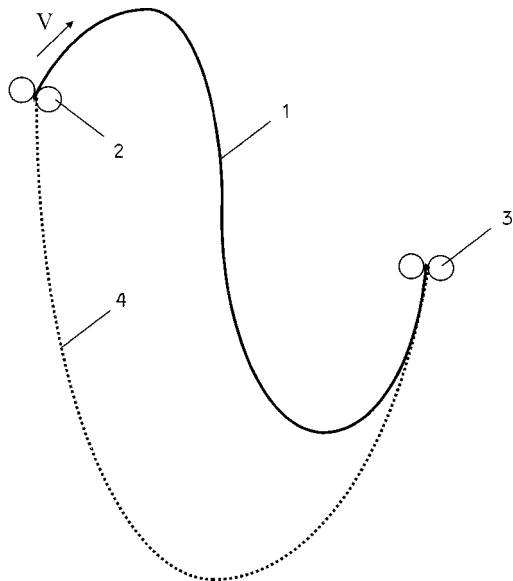


Fig. 1 Schematic illustration of the phenomenon

$$\frac{d}{dx} \left[(C_1+x) \frac{dy}{dx} \right] - \frac{dy}{dx} - n \sqrt{1 + \left(\frac{dy}{dx} \right)^2} = 0. \quad (4)$$

Separating variables and integration of Eq. (4) leads to

$$\frac{dy}{dx} = -\frac{1}{2} \left[\frac{|C_1+x|^{1+n}}{C_2} - \frac{C_2}{|C_1+x|^n} \right]. \quad (5)$$

Additional integration gives

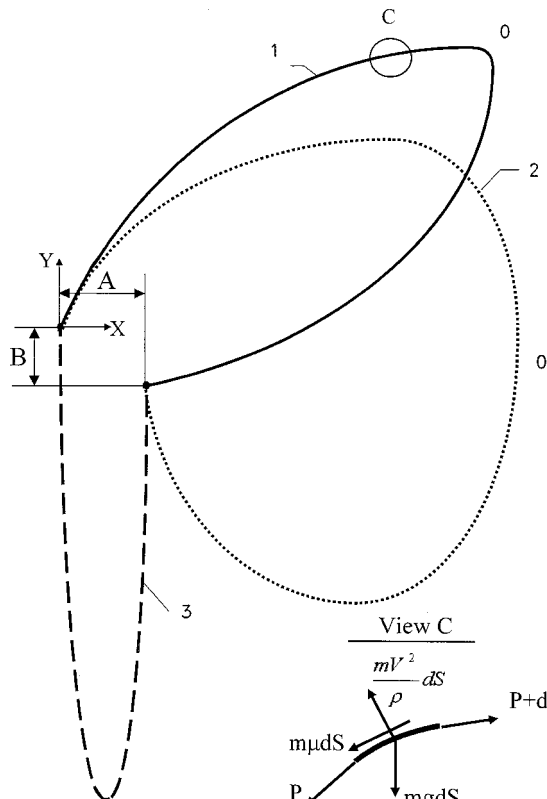


Fig. 2 Three kinds of steady-state string motion

$$y = \frac{1}{2} \left[\frac{|C_1+x|^{1+n}}{C_2(1+n)} - \frac{C_2|C_1+x|^{1-n}}{1-n} \right] + C_3. \quad (6)$$

The values p^* and s are found from Eqs. (3)–(6) after manipulations:

$$p^* = -\frac{1}{2} \left[\frac{|C_1+x|^{1+n}}{C_2} + C_2|C_1+x|^{1-n} \right], \quad (7)$$

$$s = \frac{1}{2} \left[\frac{|C_1+x|^{1+n}}{C_2(1+n)} + \frac{C_2|C_1+x|^{1-n}}{1-n} \right] + C_4, \quad (8)$$

where C_1, C_2, C_3, C_4 are arbitrary constants.

Equation (7) has a singular point at $x = -C_1$, where the “tension” p^* either vanishes or is infinite regardless of the boundary conditions. At this point the tangent to the string mode is always perpendicular to the X-axis ($dy/dx = \infty$). Evidently, the solutions (6)–(8) exist at the singularity only for the case $n < 1$.

We name the minimum velocity for which the solution exists at the singularity as the first critical velocity. This velocity V_{1cr} is found from

$$\mu(V_{1cr}) = g \quad (n=1). \quad (9)$$

Substituting Eq. (5) into

$$\rho = \frac{\left[1 + \left(\frac{dy}{dx} \right)^2 \right]^{3/2}}{\frac{d^2y}{dx^2}} \quad (10)$$

allows one to find the radius of curvature ρ

$$\rho = \pm \frac{|C_1+x|^{1+2n} + C_2^4|C_1+x|^{1-2n} + 2C_2^2|C_1+x|}{4nC_2^2}. \quad (11)$$

Investigation of Eq. (11) shows that the curvature radius can either vanish or become infinite at the singularity. We name the minimum velocity for which the curvature radius vanishes at the singularity as the second critical velocity. This velocity V_{2cr} is found from

$$\mu(V_{2cr}) = 2g \quad (n=0.5). \quad (12)$$

Thus, there are three domains of the string motion:

- subcritical, when $0 < V < V_{1cr}, 0 < \nu < 1, n > 1, \mu < g$,
- supercritical, when $V_{1cr} < V < V_{2cr}, 1 < \nu < 2, 0.5 < n < 1, g < \mu < 2g$, and
- hypercritical, when $V > V_{2cr}, \nu > 2, n < 0.5, \mu > 2g$,

where the parameter $\nu = 1/n$.

4 Subcritical String Motion

First we examine the string having a traveling velocity smaller than the first critical one (in subcritical domain). In this case as it follows from the abovementioned domain the string mode cannot contain the singularity.

When the origin of Cartesian coordinates is located at the outlet, the boundary conditions are

$$y(0) = 0; \quad y(a) = b; \quad s(0) = 0; \quad s(a) = 1, \quad (13)$$

where $a = A/L, b = B/L; A, B$ are the horizontal and vertical distances between the outlet and the inlet.

Substitution of Eqs. (6) and (8) into Eq. (13) and manipulation give the equation of the constant C_1

$$\begin{aligned} & [|C_1+a|^{1+n} - |C_1|^{1+n}] [|C_1+a|^{1-n} - |C_1|^{1-n}] \\ &= (1-b^2)(1-n^2). \end{aligned} \quad (14)$$

After numerical finding of C_1 from (14), the constants C_2, C_3 , and C_4 are calculated as follows:

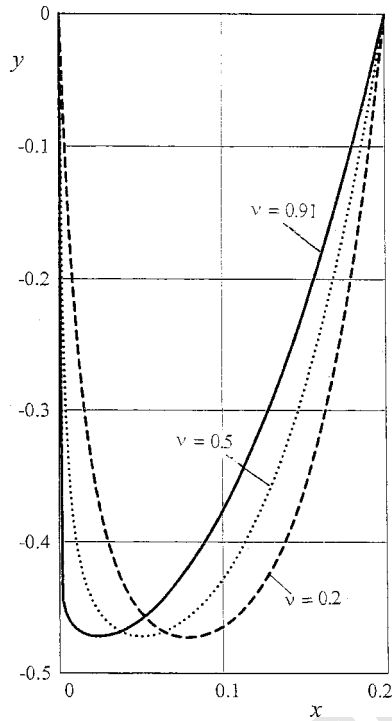


Fig. 3 The theoretical string modes for subcritical velocities

$$C_2 = \frac{(1-b)(1-n)}{|C_1+a|^{1-n} - |C_1|^{1-n}}; \quad (15)$$

$$C_3 = -\frac{1}{2} \left[\frac{|C_1|^{1+n}}{C_2(1+n)} - \frac{C_2|C_1|^{1-n}}{1-n} \right]; \quad (16)$$

$$C_4 = -\frac{1}{2} \left[\frac{|C_1|^{1+n}}{C_2(1+n)} + \frac{C_2|C_1|^{1-n}}{1-n} \right]. \quad (17)$$

The influence of traveling velocities' on string modes in the subcritical domain is presented in Fig. 3. The modes are shown for $a=0.2, b=0$. The analysis shows that the modes do not practically differ from the catenary (motionless equilibrium mode) starting from $v < 0.2$.

The plots of the nondimensional tension p^* versus nondimensional arc coordinate s for the modes of Fig. 3 are presented in Fig. 4. The analysis shows that the "tension" tends to the one of the catenary, when the traveling velocity vanishes (i.e., the parameter v approaches 0).

5 Super and Hypercritical String Motions

Now we examine the string having the traveling velocity greater than the first critical one (i.e. super and hypercritical domains). In this case the mode with the singularity, for which the "tension" vanishes, may exist. The continuous "tension" which is positive at the inlet becomes negative at the outlet.

The singular point divides the mode into two parts. In a general case the arbitrary constants C_1, C_2, C_3, C_4 in Eq. (5)–(8) may be different for each part. The arbitrary constants of the first mode part, which is located between the outlet and singularity, are lettered by subscripts "' and the ones of the second part—by subscripts "''". Using the continuity conditions at the singularity, one can obtain

$$C'_1 = C''_1 = C_1; \quad C'_3 = C''_3 = C_3; \quad C'_4 = C''_4 = C_4; \quad C'_2 \neq C''_2. \quad (18)$$

The derivative dx/dy is always infinite at the singularity regardless of the boundary conditions, therefore, the differing con-

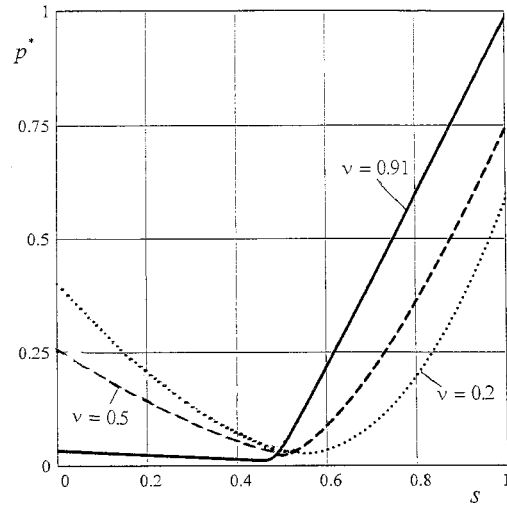


Fig. 4 The theoretical string tension for subcritical velocities

stants C'_1, C''_2 satisfy the derivative continuous condition. Thus, there are four boundary conditions (13) for determining of five constants $C_1, C'_2, C''_2, C_3, C_4$. The deficient boundary condition can be found when considering the string equilibrium in the outlet vicinity (on its both sides). One can prove that due to the negative "tension" the outlet cannot "break" the string direction. Consequently, the deficient conditions is

$$\frac{dy}{dx}(0) = \tan \alpha \quad (19)$$

where α is the known starting angle between the axis X and string outlet tangent. This angle is determined by the given direction of the outlet. Experiments also confirm the strong influence of the starting angle on the string mode.

Substitution of Eq. (5), (6), and (8) into the boundary conditions (13) and (19) permits to find five arbitrary constants $C_1, C'_2, C''_2, C_3, C_4$

$$C_1 = \frac{(1-b^2)(1-n^2) - a^2}{2a - (1+b)(1+n)\tan\left(\frac{\pi - \alpha}{4} - \frac{\alpha}{2}\right) - (1-b)(1-n)\cot\left(\frac{\pi - \alpha}{4} - \frac{\alpha}{2}\right)}; \quad (20)$$

$$C'_2 = -|C_1|'' \tan\left(\frac{\pi - \alpha}{4} - \frac{\alpha}{2}\right); \quad (21)$$

$$C''_2 = \frac{C'_2|C_1|^{1-n} + (1-b)(1-n)}{|C_1+a|^{1-n}}; \quad (22)$$

$$C_3 = -\frac{1}{2} \left[\frac{|C_1|^{1+n}}{C'_2(1+n)} - \frac{C'_2|C_1|^{1-n}}{1-n} \right]; \quad (23)$$

$$C_4 = -\frac{1}{2} \left[\frac{|C_1|^{1+n}}{C'_2(1+n)} + \frac{C'_2|C_1|^{1-n}}{1-n} \right]. \quad (24)$$

There are four solutions for the examined problem satisfying the given boundary conditions due to signs "±" in Eq. (3) and two possible values (roots) of C'_2 (in the process of Eq. (21) derivation). These solutions are shown schematically in Fig. 5. Modes 1, 2 correspond to the plus sign in Eq. (3) while modes 3, 4 correspond to the minus sign. Modes 2, 4 have mutually intersecting parts and are not of practical interest. Mode 3 can be built by setting the starting angle 180 deg greater than in mode 1.

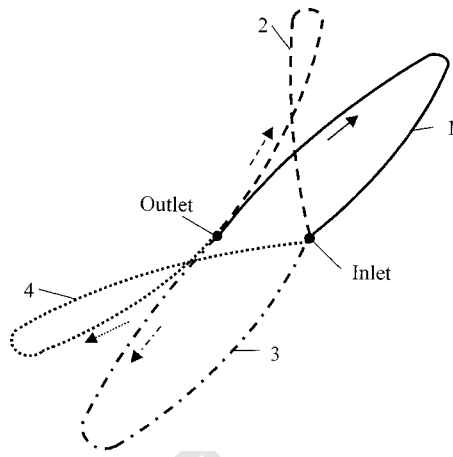


Fig. 5 The four possible solutions satisfying the given boundary conditions

Thus, only the plus sign in Eq. (3) and defined value C_2' (Eq. (21)) are considered in the paper. Corresponding string mode 1 is similar to the experimentally observed one. This mode having the singularity at positive x , may exist, if the constant C_1 is negative, thereby leading to the inequality

$$\frac{(1-b^2)(1-n^2)-a^2}{2a-(1+b)(1+n)\tan\left(\frac{\pi}{4}-\frac{\alpha}{2}\right)-(1-b)(1-n)\cot\left(\frac{\pi}{4}-\frac{\alpha}{2}\right)} < 0. \quad (25)$$

Thus, the motion with the velocity greater than the first critical one exists if its parameters n , a , b , and α satisfy the inequality (25).

The string modes in Fig. 6 correspond to velocities, which are slightly greater than the first critical one. The modes with veloci-

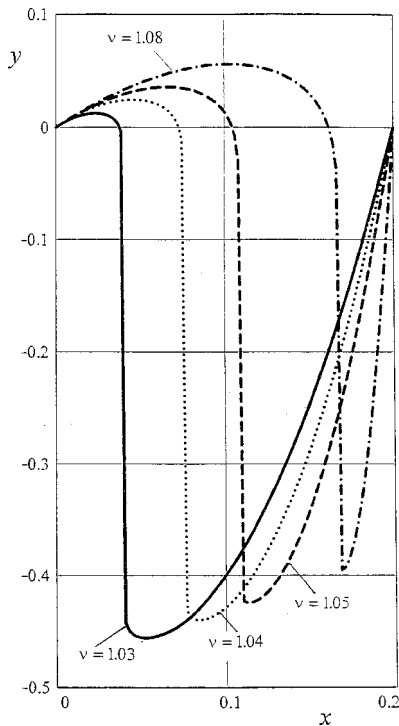


Fig. 6 The theoretical string modes ($\alpha=45$ deg) for small super-critical velocities

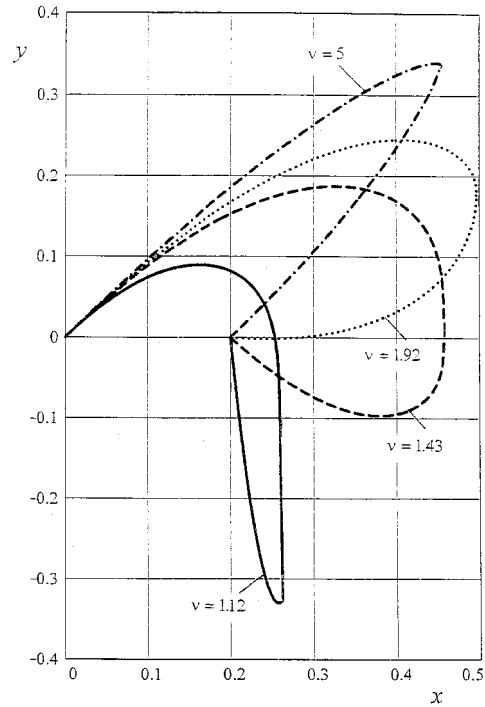


Fig. 7 The theoretical string modes ($\alpha=45$ deg) for large super and hyper critical velocities

ties which are considerably greater than the first critical velocity are presented in Fig. 7. All the modes in Figs. 6 and 7 have the starting angle $\alpha=45$ deg and parameters $a=0.2$, $b=0$.

Outlet and inlet can be assumed coinciding ($a=b=0$), when the distance between them is considerably greater than the length L . The influence of the starting angle on the modes having constant velocity ($\mu=21$ m/sec²) is shown in Fig. 8 for this case.

The string modes are experimentally determined using the experimental apparatus illustrated in Fig. 9. The closed cylindrical woven textile cord 1 which has weight/length 4.5 g/m, length 7 m, and diameter 4 mm wraps around flanged pulley 2 with the diameter 0.2 m. A surgical groove in the pulley perimeter increases the pulley-cord friction. The cord is pressed to the pulley by pinch rollers 3 and 4. The location of rollers 3 and 4 can be changed and then fixed along the pulley's circumference. The pulley attached to a DC motor moves the cord. The experiments were carried out with velocities up to 30 m/sec, which were measured with a stroboscope. A simple camera photographed the cord modes.

The comparison between theoretical and experimental modes (the theoretical ones are dotted) is presented in Figs. 10 and 11. The modes with constant velocity $V=19.6$ m/sec ($\mu=28.2$ m/sec²) and different starting angles are presented in Fig. 10. The modes with constant starting angle $\alpha=45$ deg and different velocities are shown in Fig. 11. The theoretical plots of "tension" p^* versus coordinate s , corresponding to the modes of Figs. 10, and 11, are shown in Figs. 12 and 13 accordingly.

The "equilibrium" of free string part is considered in Fig. 14 for which the weight mgL and drag force $m\mu$ of unit mass and end (outlet, inlet) "tension" forces P_1^* , P_2^* load the string. The equilibrium of moments with respect to the intersection point O of the end forces' directions gives

$$gLd = \mu\Omega, \quad (26)$$

where Ω is the corresponding area of the mode; d is the distance between the center of gravity of the mode's area and point of end forces' intersection.

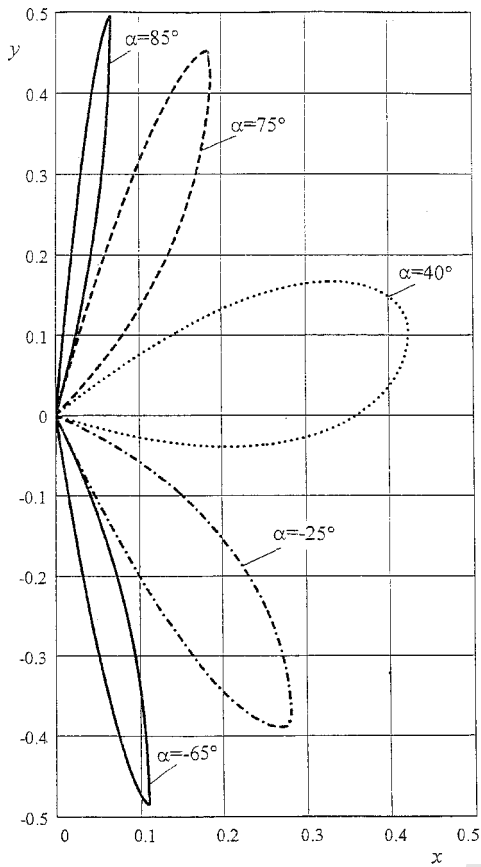


Fig. 8 The theoretical string modes ($\mu=21 \text{ m/sec}^2$) for different starting angles

Equation (26) enables to find the drag force acceleration μ from Eq. (26) when the experimental string mode is known.

3 Discussion of Results

As shown above there are three kinds of string modes (Fig. 2):

- falling mode 3 without the singularity (in the subcritical domain);
- roundish mode 2 with the singularity when the radius of curvature at the singularity is infinite (in the supercritical domain); and
- extended, sharp at the top mode 1 with the singularity when the radius of curvature at the singularity vanishes (in the hypercritical domain).

The boundary conditions for the subcritical motion are the same as for the motionless string equilibrium because there is no singularity. The singularity leads to an additional boundary condition at the outlet. The modes strongly depend on the solution behavior at

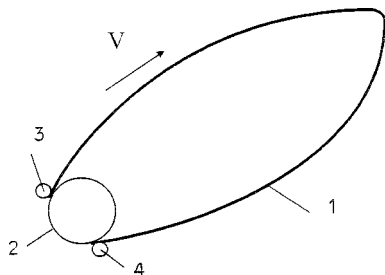


Fig. 9 The schematic diagram of experimental apparatus

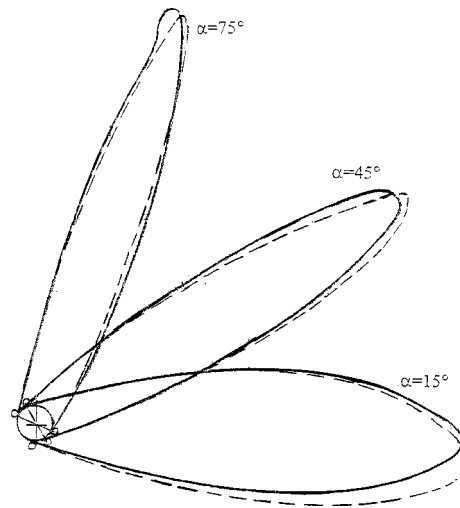


Fig. 10 The theoretical and experimental modes ($\mu=28.3 \text{ m/sec}^2$) for different start angles

the singularity. The supercritical motion may occur only if the solution exists at the singularity. The conditions for existence of the solution are derived for unlimited string length. However, string stability and strength, motor power, etc. limit the length. This issue is a separate subject for investigation that is not considered in the paper.

The analogy between the steady-state motion and equilibrium is also interesting. The equilibrium equations of any mode part may be written (as though the string does not travel) when changing the real tension P to the fictitious one $P^* = P - mV^2$.

The phenomenon's existence may be explained while considering the momentum "equilibrium" of the string part which is shown in Fig. 14. The string does not "fall" under the weight influence because the moment of the drag force balances the moment of the weight. One should pay attention to the paradox of negative value of the "tension" p_1^* in the equilibrium, despite the fact that the real tension P_1 is always positive.

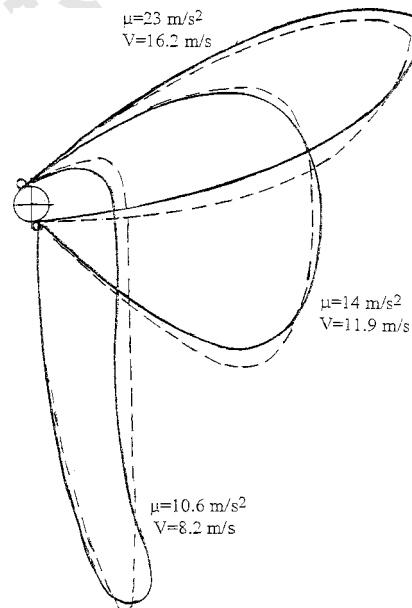


Fig. 11 The theoretical and experimental modes ($\alpha=45 \text{ deg}$) for different velocities

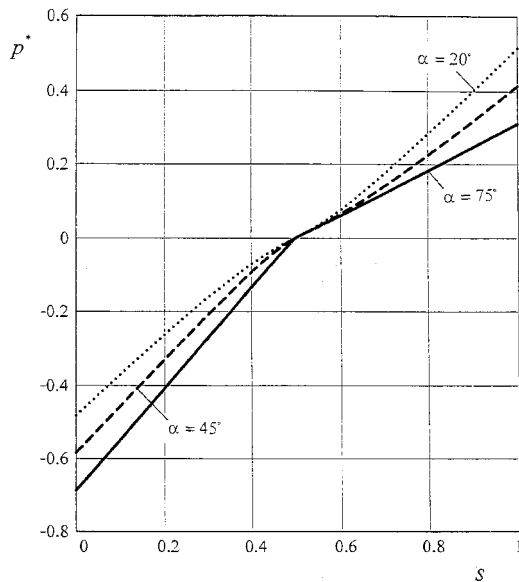


Fig. 12 The theoretical string tension for the modes of Fig. 9

Figures 3, 6, and 7 show the string elevation starting from the catenary, as the longitudinal velocity increases. The tension changes along with velocity as shown in Fig. 5. The modes and tension that correspond to small traveling velocity are close to the ones of the catenary. Figure 8 shows strong dependence of modes on the starting angle.

Theoretical modes agree well with experimental ones. This agreement may be explained by minimum of assumptions that are made at the transition from the real string to its mathematical model. The experiments also show that the string “falls” when the condition (25) is not satisfied. This may occur, for example, if the starting angle or the distance between the outlet and inlet is changed.

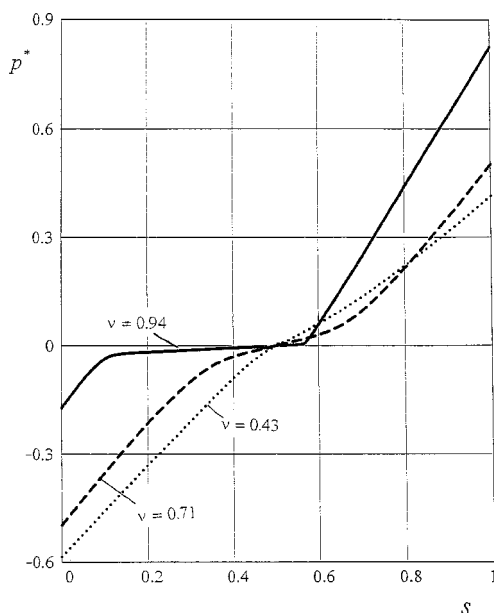


Fig. 13 The theoretical string tension for the modes of Fig. 10

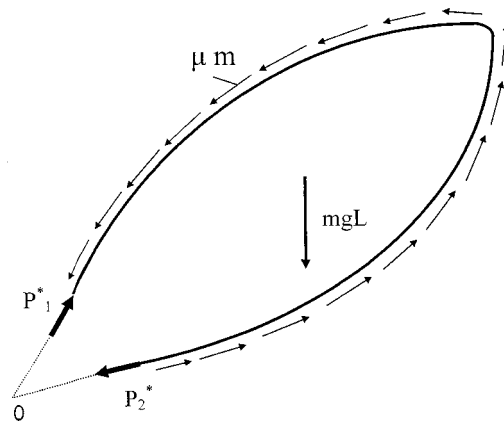


Fig. 14 The explanation of the phenomenon's existence

Acknowledgment

The author acknowledges his daughter Elena for her aid in editing of this paper.

Appendix

Derivation of Differential Equations of Steady-State String Motion. We write planar dynamic equations for an element of homogeneous, ideally flexible string without bending and torsional stiffness. The string travels with a constant velocity along an invariant mode

$$m \frac{\partial \bar{V}}{\partial t} = \frac{\partial \bar{Q}}{\partial S} - \bar{q} \tag{27}$$

where $\bar{V} = V\bar{e}_1$ is the string velocity vector having the module V and directed along the tangent to the mode unit vector \bar{e}_1 ; $\bar{Q} = T\bar{e}_1$ is the cross-section string force vector which is directed along the unit vector \bar{e}_1 ; T is the string tension; \bar{q} is the vector of distributed linear external force acting on string; m is the string linear mass; t is the time; and S is the arc coordinate along the string mode.

Performing differentiation with respect to coordinate S when taking into consideration that $\partial S / \partial t = V = \text{const}$ gives

$$\frac{\partial \bar{V}}{\partial t} = \frac{\partial \bar{V}}{\partial S} \frac{\partial S}{\partial t} = V^2 \frac{\partial \bar{e}_1}{\partial S} \tag{28}$$

Substitution of Eq. (28) into Eq. (27) in terms of

$$\frac{\partial \bar{Q}}{\partial S} = \frac{\partial (T\bar{e}_1)}{\partial S} = \frac{\partial T}{\partial S} \bar{e}_1 + T \frac{\partial \bar{e}_1}{\partial S} \tag{30}$$

while using total derivatives instead of partial ones (the string mode does not depend on time) and manipulations lead to

$$(T - mV^2) \frac{d\bar{e}_1}{dS} + \frac{d(T - mV^2)}{dS} \bar{e}_1 + \bar{q} = 0 \tag{31}$$

Applying of variable $T^* = T - mV^2$ gives

$$\frac{\partial \bar{T}^*}{\partial S} + \bar{q} = 0 \tag{32}$$

where $\bar{T}^* = T^* \bar{e}_1$.

Equation (32) is almost identical to the equation of the string equilibrium with difference in use of fictitious tension T^* instead of the real one T . This allows one to apply Eq. (32) as equilibrium equation for an arbitrary string part.

We obtain the equations in projections onto Cartesian coordinates X, Y using Eq. (32) and relations for “tension” projections T_X^* and T_Y^*

$$T_X^* = T^* \frac{dX}{dS}; \quad T_Y^* = T^* \frac{dY}{dS}. \quad (33)$$

The third equation necessary for solution is the relation between the cosines

$$\frac{d}{dS} \left(T^* \frac{dX}{dS} \right) + q_X = 0;$$

$$\frac{d}{dS} \left(T^* \frac{dY}{dS} \right) + q_Y = 0; \quad (34)$$

$$\left(\frac{dX}{dS} \right)^2 + \left(\frac{dY}{dS} \right)^2 = 1$$

where q_X and q_Y are the projections of the distributed external force.

References

- [1] Aitkin, J., 1878, “An Account of Some Experiments on Rigidity Produced by Centrifugal Forces,” *Philos. Mag.*, **5**.
- [2] Radinger, G., 1878, *Dampfmaschinen*, **5**.
- [3] Smith, W. E., and Weathezchon, R. C., 1961, “A New Type of Thermal Radiator of Space Vehicle,” *ARS*, **20**, No. 1, pp. 32–36.
- [4] Burge, H., 1962, “Revolving Bolt Space Radiator,” *ARS*, **32**, No. 8, pp. 17–25.
- [5] Voevodin, A. A., 1965, “Dynamic Equilibrium of Closed String in Earth Conditions,” *Proceedings of USSR Connection department*, Vol. 2, pp. 89–108.
- [6] Kurkin, V. I., and Lebedev, I. P., 1965, “Calculation of String Air Resistance,” *Izvestia Vuzov, Tehnologiya Tekstilnoi Prom.*, **1**, M., pp. 166–169.
- [7] Svetlicky, V. A., and Gabruk, V. I., 1966, “Critical Velocities of the Steady State Motion,” *Soviet Applied Mechanics*, **6**, pp. 13–17.
- [8] Cohen, H., and Epstein, M., 1994, “On a Class of Planar Motions of Flexible Rods,” *ASME J. Appl. Mech.*, **61**, pp. 206–208.
- [9] Nordenholz, T. R., and O’Reilly, O. M., 1995, “On Kinematical Conditions for Steady Motion of Strings and Rods,” *ASME J. Appl. Mech.*, **62**, pp. 820–822.
- [10] Svetlicky, V. A., and Miroshnik, R. A., 1972, “Critical Velocities of the Steady State Motion of an Elastic Fiber in a Planar Homogeneous Flow,” *Soviet Applied Mechanics*, **6**, pp. 52–57.
- [11] Kurkin, V. A., and Miroshnik, R. A., 1988, “The Spatial Stationary Movement of the Heavy Perfectly Flexible Bar,” *Soviet Applied Mechanics*, **24**, pp. 113–116.
- [12] Healey, T. J., and Papadopoulos, J. N., 1990, “Steady Axial Motion of Strings,” *ASME J. Appl. Mech.*, **57**, pp. 785–787.
- [13] Schagerl, M., Steiner, W., and Troger, H., 1997, “On the Paradox of the Free Falling Folded Chair,” *Acta Mech.*, **125**, pp. 155–168.
- [14] Perkins, N. C., and Mote, C. D., Jr., 1987, “Three-Dimensional Vibration of Travelling Elastic Cables,” *J. Sound Vib.*, **114**, No.2, pp. 305–340.
- [15] Perkins, N. C., and Mote, C. D., Jr., 1989, “Theoretical and Experimental Stability of Two Translating Cable Equilibria,” *J. Sound Vib.*, **128**, No. 3, pp. 397–410.